Biochemistry

 Volume 29, Number 14 April 10, 1990

Articles

Dynamics in Synthetic Oligonucleotides. A Solid-State Deuterium NMR Study†

Todd M. Alam and Gary Drobny*
Department of Chemistry, University of Washington, Seattle, Washington 98195
Received August 3, 1989; Revised Manuscript Received November 28, 1989

ABSTRACT: Solid-state ^2H NMR spectroscopy was used to investigate dynamics in the [*methyl*-^2H]thymidine-labeled oligonucleotide [d(CGCGAAT*T*CGCG)]$_2$. Quadrupole echo line shapes, spin–lattice relaxation, and quadrupolar echo decay rates were investigated as a function of hydration **W** (moles of water/moles of nucleotide) between 0 and ~30. The amplitude of the base motion, modeled as a fast four-site libration, or diffusion in a cone, increased slightly with higher levels of hydration. A slower component of motion about the helix axis appears at **W** ~ 10 and increases in rate and amplitude, leading to the intermediate rate line shape observed at **W** ~ 21.

The role of dynamics in the cellular function of polynucleotides has spurred numerous experimental and theoretical investigations of internal motions in nucleic acids (Barkley & Zimm, 1979; Allison & Schurr, 1979; Langowski et al., 1985; Schurr & Fujimoto, 1988; Lipari & Szabo, 1981a; Hogan & Jardetzky, 1979, 1980; Opella et al., 1981). In particular, there have been a large number of high-resolution NMR[1] investigations of DNA dynamics from relaxation data, with the objective of elucidating the exact nature of internal dynamics occurring in DNA [for a review see James (1984)]. Many of the investigations, notably work by Hogan and Jardetzky (1979, 1980), Bolton and James (1979, 1980), and Bendel et al. (1982), have reported large-amplitude internal motions with correlation times in the neighborhood of nanoseconds. Analysis of relaxation data including contributions of collective torsional motions has suggested that the amplitude of local internal motion may not be as large as previously supposed (Allison et al., 1982). It is evident that there still remains some controversy concerning the nature of motions in DNA, as well as the contributions of local and collective motions.

Solution NMR studies suffer from the disadvantage that information concerning the anisotropic nature of spin interactions is lost due to isotropic averaging from molecular tumbling. As a consequence, dynamical information must be obtained through an analysis of NMR relaxation data, in particular spin–lattice (T_1) and spin–spin (T_2) relaxation. Interpretation of spin–lattice relaxation in systems of dipolar coupled nuclei (i.e., ^1H, ^{31}P) can be a very complicated process, invariably requiring numerous assumptions of local geometry and relaxation mechanisms. This is especially true with ^{31}P relaxation data where an analysis requires inclusion of not only dipolar terms in T_1 but also CSA and possibly dipolar/CSA cross terms.

In solid-state NMR retention of anisotropic spin interactions allows dynamical information to manifest itself within the spectral line shape, which is sensitive to both the rate and the type of motion (Davis, 1983; Spiess, 1985; Opella, 1986). Investigation of relaxation in solid-state NMR also provides a probe of the rate and type of motion occurring within the molecule (Torchia & Szabo, 1982). Solid-state NMR has found application in the study of DNA, including numerous investigations using ^{31}P NMR to probe the dynamics of the phosphorus backbone [for a review see Shindo (1984)], along with ^7Li and ^{23}Na NMR studies of oriented DNA (Edzes et al., 1972; Kowalewski et al., 1988; Einarsson et al., 1990).

Deuterium NMR, which has been used extensively to study polymer systems, possesses several advantages as a dynamic probe. First, the quadrupole interaction dominates both the spectral line shape and the relaxation of deuterons, and because this interaction is a single nucleus property, no detailed

† This research was supported by NIH Program Project Grant (GM 32681-06) and the NIH Molecular Biophysics Grant to T.M.A. (GM 08268-02).

[1] Abbreviations: NMR, nuclear magnetic resonance; CSA, chemical shift anisotropy; NOE, nuclear Overhauser effect; PAGE, polyacrylamide gel electrophoresis; EFG, electrical field gradient; PAS, principal axis system; FID, free induction decay; RH, relative humidity; RI, relative intensity.

0006-2960/90/0429-3421$02.50/0

structural information is required to invoke it as a relaxation mechanism. In addition, the dynamic range of motions that may be studied by deuterium NMR is very high, ranging from 10^3 to 10^{10} Hz.

Solid-state ^{2}H NMR investigations of nucleic acids have dealt primarily with base dynamics of DNA, but there has been recent work involving the sugar 2′,2′-dideuteriodeoxyguanosine and 2′,2′-dideuteriothymidine (Roy et al., 1986), as well as 2″-deuteriodeoxyadenosine and its incorporation into a synthetic oligonucleotide (Huang, 1989; Huang et al., 1990). There have also been studies involving the 5′,5′-dideuteriothymidine (Kintanar et al., 1988), along with the interesting ^{2}H studies of hydration waters in solid Li–DNA (Brandes et al., 1988b) and magnetically ordered DNA liquid crystals (Brandes & Kearns, 1986).

In an early ^{2}H study of base dynamics in solid B-form DNA (DiVerdi & Opella, 1981) no fast, large amplitude motions of the bases were detected as a function of temperature. Investigation of the base dynamics as a function of hydration have shown small but significant librational motions that increase with higher water content. In the study of poly(I) and poly(I)·poly(C) fibers (Bendel et al., 1983; James et al., 1983) an increase in hydration to approximately eight waters per nucleotide showed an increase in minimum fluctuations described by a cone of half-angle θ for the double-stranded sample from $\theta \sim \pm 1.9°$ to $\theta \sim \pm 2.4°$ and near complete loss of the quadrupolar echo at elevated hydrations, suggesting the presence of motions in the microsecond range. Deuterium NMR studies on oriented and unoriented sodium and lithium calf thymus DNA as a function of hydration have also been reported (Vold et al., 1986; Brandes et al., 1986, 1988a). In these studies the hydration level ranges through ~22 waters per nucleotide, resulting in a significant increase in the amplitude of local motions with elevated water content. By use of a four-site librational model the maximum base amplitude was $\sim \pm 10°$ at low hydration levels, and at 14 waters per nucleotide the base librations increase to $\sim \pm 14°$. At higher humidity levels the onset of slower motions results in the complete loss of the quadrupolar echo. Recent investigation of the spectral densities $J_1(\omega_0)$ and $J_2(2\omega_0)$ of oriented Li–DNA allows insight into the internal motions of polynucleotides, but also hints at the complexity of such motions (Brandes et al., 1990). In a similar study of salmon sperm DNA films and oriented fibers, base fluctuations modeled as a four-site libration increased from approximately ±8.5° at 79% relative humidity (RH) to ±13.5° at 92% RH. At these higher hydrations a slower motion about the helix axis was observed (rms fluctuations 30° and $\tau_c \sim 10^{-6}$ s) in both the ^{2}H and ^{31}P studies (Fujiwara & Shindo, 1985; Shindo et al., 1987). Solid-state ^{2}H NMR studies of base motion within well-defined synthetic oligonucleotides have also recently been reported (Kintanar et al., 1989). The amplitudes of base librations reported are very similar to those of previous hydration studies, including the appearance of a slower motion at 80% RH, with $\tau_c \sim 10^{-6}$ s.

In this study the internal dynamics of the synthetic DNA dodecamer [d(CGCGAAT*T*CGCG)]$_2$ are investigated by using [*methyl*-^{2}H]thymidine incorporated into positions dT7 and dT8. This self-complementary dodecamer contains the *Eco*RI restriction endonuclease recognition site d(GAATTC) and has been extensively studied in both the liquid and crystalline states. For instance, this sequence was the first oligonucleotide single crystal investigated containing a complete turn of double-helical B-form DNA and has been the subject of several X-ray diffraction investigations (Wing et al., 1980; Dickerson & Drew, 1981a,b; Kopka et al., 1985; Pjura et al., 1987). In addition, information on the dynamics and local mobility within the crystal have been obtained from isotropic thermal factors (Drew et al., 1981) and segmented rigid body analysis (Holbrook & Kim, 1984). Studies involving the geometry of hydration have also been performed (Drew & Dickerson, 1981; Kopka et al., 1983). The sequence was also investigated by using high-resolution two-dimensional NMR (Hare et al., 1983), and a structure has been obtained from NOE data through distance geometry methods (Nerdal et al., 1989), along with a preliminary investigation of sugar conformation (Bax & Lerner, 1988).

We have acquired quadrupolar echo line shapes, spin–lattice relaxation times (T_1), and quadrupolar echo decay times (T_{2e}) as a function of hydration, allowing the development of a motional model to describe the internal dynamics in oligonucleotides. In this study, however, we have primarily exploited the changes of spectral line shape in the analysis of molecular motion. The dominant motion occurring is the fast reorientation of the methyl group about the C_3 symmetry axis, but as we will show, other dynamics manifest themselves within the observed spectral line shape. Since the methyl group is rigidly attached to the pyrimidine base, it is influenced by base dynamics as well as overall molecular dynamics. Due to the partial averaging by the methyl motion, the line shape is sensitive to motions on a slower time scale than those of previous base-labeled materials. The results are compared to previous base studies, and a motional model is presented.

To understand the line-shape analysis, a brief review of general deuterium NMR theory is presented. For an isolated deuteron in a solid, the NMR frequency is given by

$$\omega = \omega_0 \pm \omega_Q$$

where

$$\omega_Q = 3\pi/4(e^2qQ/h)[3\cos^2\Theta - 1 - \eta\sin^2\Theta\cos 2\Phi]$$

(e^2qQ/h) is the quadrupolar coupling constant (QCC), and η is the asymmetry parameter that describes the deviation from cylindrical symmetry of the electrical field gradient (EFG) tensor about the q_{zz} axis in the principal axis system (PAS). The orientation of the magnetic field $\mathbf{B}_0$ in the PAS of the EFG tensor is described by the polar angles Θ and Φ (Abragam, 1961). In the presence of motion the ^{2}H NMR line shape will change. If the molecular motion is rapid on the time scale of ω_Q^{-1}, the frequency can be defined by using QCC_{eff} and η_{eff}, the effective quadrupolar coupling constant and asymmetry parameter of the averaged electrical field gradient, respectively. If the motion occurs within the intermediate exchange regime ($\sim\omega_Q^{-1}$), the use of QCC_{eff} and η_{eff} is not applicable, and it becomes necessary to calculate the spectrum for continuous dynamics with a diffusion operator or discrete dynamics utilizing a jump matrix, where the modulation effect of molecular motion on the angular dependent frequencies is determined. These types of analysis have been previously discussed (Barbara et al., 1986; Wittebort et al., 1987).

Materials and Methods

Labeled Synthesis. Labeled [*methyl*-^{2}H]thymidine was prepared by using a scaled procedure previously described (Kintanar et al., 1988). The purity and extent of deuterium incorporation in the labeled compound was determined by high-resolution ^{1}H NMR spectroscopy at 500 MHz, which indicated greater than 75% exchange at the methyl position and less than 5% exchange at the H6 base position; no impurities were detected. The reduction in percent deuteration in contrast to previous studies is most likely the result of

Table I: Line-Shape Parameters and Relaxation Rates of [d(CGCGAAT*T*CGCG)]$_2$[a]

RH (%)	W	RI (%)	QCC_{eff} (kHz)	η_{eff}	$\langle T_1 \rangle$ (ms)	$\langle T_{2e} \rangle$ (μs)	$\langle T_{2e} \rangle^b$ (μs)
dry	0.0	1.00	51.5 ± 0.5	0.05	357 ± 23	396 ± 45	
66	5.0	0.99	51.5 ± 0.5	0.05	260 ± 13	316 ± 31	
75	10.4	0.86	51.0 ± 0.5	0.05	204 ± 10	252 ± 25	250
80	11.6	0.80	50.5 ± 0.5	0.05	213 ± 11	244 ± 23	250
88	16.3	0.40	45.5 ± 0.5	0.06	173 ± 12	142 ± 20	135
90	21.2	0.43	[c]	[c]	161 ± 08	115 ± 10	163
92	26.6	0.62	20.5 ± 0.5	~0	146 ± 07	200 ± 18	218
92	29.6	0.79	20.0 ± 0.5	~0	127 ± 06	230 ± 20	213
95	39.8	0.60	15.0 ± 0.5	~0	103 ± 06	249 ± 24	256
98	69.9		~0[d]	~0[d]			

[a] Experiments performed at 298 K. [b] Calculated value. [c] Intermediate rate line shape. [d] Observed only isotropic component.

incomplete exchange during scale up.

The deuterated β-cyanoethyl phosphoramidite was prepared by using the following procedure. Labeled thymidine was protected at the 5′-position with 4,4′-dimethoxytrityl (DMT) according to established procedures (Ti et al., 1982). The 5′-*O*-DMT-[*methyl*-^{2}H]thymidine was converted to the corresponding 3′-(*O*-β-cyanoethyl *N*,*N*-diisopropylphosphoramidite) by procedures described previously in the preparation of [H6-^{2}H]thymidine phosphoramidite (Barone et al., 1984; Kintanar et al., 1989). The only modification was the addition of 1.1 equiv of β-cyanoethyl-(*N*,*N*-diisopropylamino)phosphine[2] (Sinha et al., 1984) in place of (*N*,*N*-diisopropylamino)methoxyphosphine. The crude product was purified by flash chromatography (ethyl acetate) to yield the desired labeled phosphoramidite.

The DNA sample investigated was prepared in two 10-μmol batches by using the phosphoramidite method on an Applied Biosystems 380A DNA synthesizer. The labeled thymidine phosphoramidite was added at the appropriate step in the synthetic sequence to produce the self-complementary dodecamer [d(CGCGAAT*T*CGCG)]$_2$. Each synthesis was ethanol precipitated followed by desalting on a Sephadex G-10 column (60 cm × 2 cm). The purity and homogeneity of the DNA sample were verified by PAGE and ^{1}H NMR spectroscopy at 500 MHz. Both syntheses were greater than 95% pure (free of short failure sequences and organic contaminants) as determined by comparison to previously published ^{1}H NMR spectrum of the unlabeled sequence (Hare et al., 1983). NMR spectroscopy also confirmed that the sample was ~75% deuterated at the dT7 and dT8 positions. To the purified, desalted DNA was added 10% NaCl by weight. Labile deuterons were reexchanged by lyophilizing from ^{2}H-depleted water. The lyophilized DNA, total weight 56.5 mg, was packed into a 5 mm × 15 mm NMR tube. The sample was hydrated over appropriate salt solutions containing ^{2}H-depleted water (Weast, 1979). Equilibration for 3–4 weeks at each humidity level allowed for complete and uniform humidification, and water adsorption as a function of relative humidity was monitored gravimetrically. A blank tare was allowed to equilibrate at each humidity to determine and correct for water adsorption on glass. The difficulty in removing all the water from DNA, even with extensive pumping, has been noted (Rupprecht & Forslind, 1970), but the error introduced by the assumption that the lyophilized samples were dry is small and will result in reported hydration levels being slightly reduced from real values. Determination of the DNA dry weight allowed the calculation of water adsorption for each relative humidity, and the results are presented in Table I.

Solid-State NMR Spectroscopy. Solid-state ^{2}H spectra were obtained at 76.75 MHz with quadrature phase detection on a home-built spectrometer (Drobny and Gladden, unpublished results) controlled by a DEC MicroVaxII. An eight-step phase-cycled quadrupolar echo sequence, $\pi/2_x-\tau_1-\pi/2_y-\tau_2-$acq, with $\pi/2$ pulses less than 3 μs was used for data acquisition (Griffin, 1981). A recycle delay of $\sim 5T_1$ was used to ensure thermal (spin) equilibrium. Pulse spacing, τ_1, varied from 40 to 200 μs, while data acquisition was initiated prior to the solid echo by adjustment of τ_2. The time domain signal was left shifted to the echo maximum prior to Fourier transformation. Lorentzian line broadening of 500–1000 Hz was applied to the experimental spectrum to obtain adequate signal to noise ratios.

Deuterium spin–lattice relaxation times were determined by using an inversion recovery pulse sequence. The magnetization was determined from the echo height maximum and fit by using a nonlinear least-squares analysis (De Fontaine et al., 1975) to the exponential magnetization curve

$$S(t) = S(\infty)[1 - 2e^{-t/T_1}]$$

Relaxations obtained from the quadrupolar echo height are commonly referred to as "powder averages" and denoted as $\langle T_1 \rangle$. The irreversible loss of phase memory as a function of pulse separation, referred to as $\langle T_{2e} \rangle$, was determined from echo maximum and fit to the exponential recovery curve

$$S(2\tau_1) = Ae^{-2\tau_1/T_{2e}}$$

Line-Shape Simulations. Simulations of deuterium NMR line shapes were obtained by using the program MXQET, which can accommodate multisite, multiaxis motional models and has been described in detail elsehwere (Greenfield et al., 1987). Powder patterns and FIDs were calculated for the spectra including finite pulse corrections and effects of exchange during pulses. Aligned sample simulations were obtained by using a modified version of MXQET, allowing different distributions of the helix axis orientation. Static values of the quadrupolar coupling constant (e^2qQ/h) and the asymmetry parameters (η) were obtained from previous monomer studies (Kintanar et al., 1988). Effective values of the quadrupolar coupling constant (QCC_{eff}) and asymmetry parameter (η_{eff}) were determined from observed line shapes, assuming no motional models. The splitting between perpendicular edges ("horns"), δ, and the separation between parallel edges, Δ, have previously been used to describe motional effects on the electrical field gradient (EFG) tensor. It was found that more accurate fits could be obtained by simulation of the entire experimental powder pattern. The relationship between (QCC_{eff}), η_{eff}, and δ,Δ has been described elsewhere (Brandes et al., 1986). All simulations were run on either a DEC Vaxstation 3200 or a Convex C1.

Results

Water adsorption **W** (moles of H_2O/moles of nucleotide) as a function of relative humidity for the sodium dodecamer

[2] The gracious gift of Dr. Andreas Spaltenstein.

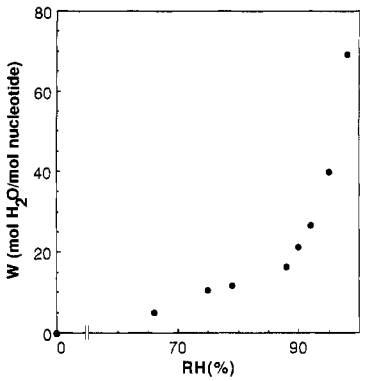

FIGURE 1: Water content, W (moles of H_2O/moles of nucleotide), of Na–[d(CGCGAAT*T*CGCG)]$_2$ with variation in percent relative humidity, RH.

is illustrated in Figure 1. The results are similar to those presented previously (Falk et al., 1962; Brandes et al., 1986). The humidity studies on the lyophilized dodecamer did reveal a slightly higher W than observed in previous investigations of oriented films or fibers, resulting from the increased amount of salt present. Water adsorption by DNA has been shown to be dependent on salt concentration (Rupprecht & Forslind, 1970).

Solid-state ^{2}H spectra, spin–lattice relaxation times $\langle T_1 \rangle$, and quadrupolar echo decay times, $\langle T_{2e} \rangle$, were obtained at 76.75 MHz for [*methyl*-^{2}H]thymidine, [d-(CGCGAAT*T*CGCG)]$_2$, as a function of relative humidity (RH) ranging from dry (W = 0.0) to 98% (W = 69.9). Effective quadrupolar coupling constants, QCC_{eff}, effective asymmetry parameters, η_{eff}, relative intensities (RI), $\langle T_1 \rangle$, and $\langle T_{2e} \rangle$ for humidities through 90% RH are given in Table I. For hydration levels above 92% RH a liquid-crystalline phase was observed and will be discussed in detail elsewhere (Alam & Drobny, 1990). Representative line shapes as a function of hydration for [d(CGCGAAT*T*CGCG)]$_2$ are presented in Figure 2.

Up to a relative humidity of 80% (W = 11.6) there are no significant changes of the observed line shape aside from a 1.0-kHz reduction in QCC_{eff}, and the effective asymmetry parameter remains constant throughout this range (Figure 2a,b). The line shape undergoes a slight loss of center intensity with increasing humidity through 88% RH. Beginning with 88% RH (W = 16.3), a 5.0-kHz reduction in QCC_{eff} with respect to 80% RH is observed followed by drastic reduction to 20.5 kHz at 92% RH (W = 26.6) and 15 kHz at 95% RH (W = 39.8) (Figure 2c,e,f). The line shape at 90% RH (W = 21.2) is uniquely a signature of intermediate rate motion occurring within the sample and therefore could not be characterized by an effective QCC or η (Figure 2d). Above W $\sim$ 25 the turbid appearance of the sample cleared when placed in the magnetic field, behavior characteristic of aligned samples. This liquid-crystalline phase has been investigated in more detail and will be presented in a subsequent paper (Alam & Drobny, 1990). Beginning at W $\sim$ 20, an isotropic component became conspicuous and increased in relative magnitude until at W = 69.9 only a central isotropic line was observed. At low hydration levels this isotropic component was attributed to residual HOD, while at higher humidity levels it may result from isotropic regions within the sample.

Increasing the level of hydration from the lyophilized powder produced a loss in relative intensity (RI) through 90% RH (W = 21.2), followed by a surprising increase in signal intensity beginning at 92% RH (W = 26.6). Similar attenuation of quadrupolar echo intensity as a function of hydration has been

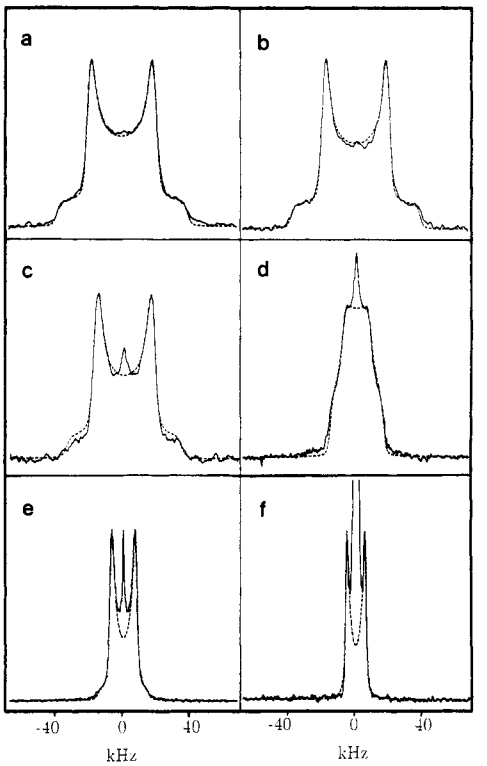

FIGURE 2: Experimental and simulated (---) 76.75-MHz deuterium quadrupole echo spectra of [*methyl*-^{2}H]thymidine-labeled [d-(CGCGAAT*T*CGCG)]$_2$ at various hydration levels W (moles of H_2O/moles of nucleotide). The simulated spectra were calculated as described in text, ignoring the central isotropic component. Spectra are shown for pulse delay of 50 μs at (a) dry lyophilized powder, W $\sim$ 0, 12 000 scans, (b) 75% RH, W = 10.4, 24 000 scans, (c) 88% RH, W = 16.3, 32 000 scans, (d) 90% RH, W = 21.2, 28 500 scans, (e) 92% RH, W = 26.6, 32 000 scans, and (f) 95% RH, W = 39.8, 8000 scans.

reported (Bendel et al., 1983; Brandes et al., 1986), resulting in the complete loss of the quadrupolar echo at hydration levels greater than 92% RH. Preliminary data at 92% RH (W = 24.9) on the base-labeled dodecamer revealed a signal with a reduction in QCC_{eff} of approximately 100 kHz, and a RI of $\sim$0.09 (Huang, 1989). Quadrupolar echo spectra of salmon sperm DNA films and oriented fibers have been reported as high as 98% RH but lacked discussion concerning the extent of relative intensity loss (Shindo et al., 1987).

Corresponding behavior of $\langle T_{2e} \rangle$ with increasing humidity was observed with a 4-fold decrease through 90% RH (W = 21.1) followed by an increase in $\langle T_{2e} \rangle$ above 92% RH (W = 26.6) (see Table I). Significant loss in signal intensity with variation in pulse delay was observed (for example, see Figure 3a for 75% RH), while anisotropic T_{2e} effects were not as pronounced as in previous studies (Brandes et al., 1986; Shindo et al., 1987; Kintanar et al., 1989). This result is not readily apparent unless the spectra are scaled to the same relative intensity (Figure 3b). The largest degree of anisotropic behavior with variation in pulse delay was observed for 90% RH.

Spin–lattice relaxation times, $\langle T_1 \rangle$, decreased by a factor of 3.5 from dry to 95% RH (W = 39.8). The most dramatic decrease occurred between the "dry" and 66% RH samples, followed by a plateau at higher hydration levels. Relaxation times for the dry sample were significantly different from those observed for the monomer [*methyl*-^{2}H]thymidine. It should be noted that the relaxation recovery curves were found to be highly nonexponential in the dry sample. The anisotropic relaxation behavior of the thymidine methyl group undergoing a 3-fold jump would be expected to give multiexponential relaxation if a powder average recovery is monitored (Torchia

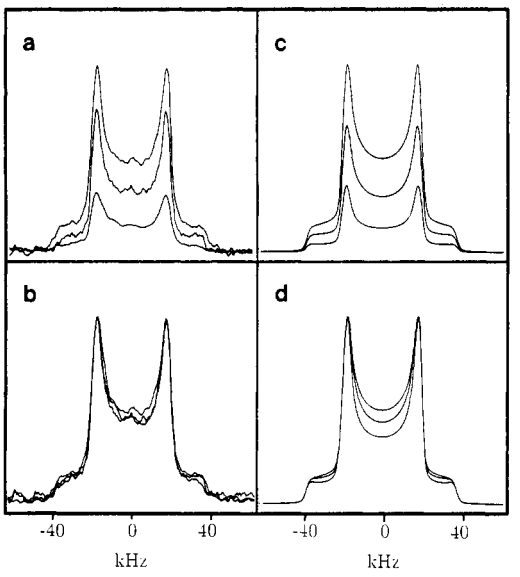

FIGURE 3: Solid-state ^2H NMR spectra of [d-(CGCGAAT*T*CGCG)]$_2$ hydrated at 75% RH, W = 10.4, with (a) variation in pulse delay of 50, 110, and 200 μs, (b) same as (a) except scaled to the same absolute intensity, (c) simulated spectra obtained from the motional model described in the text, and (d) same as (c) scaled to the same absolute intensity.

& Szabo, 1982). These deviations from a single-exponential relaxation are difficult to distinguish and were not discernible in the monomer studies (Kintanar et al., 1988). Presently the signal to noise ratio of the deuterated dodecamer and available instrumentation do not allow a thorough analysis of the anisotropic behavior of T_1 within the dodecamer, and for this reason powder average $\langle T_1 \rangle$s were determined and anisotropic effects ignored. The dry sample relaxation data were subsequently fit by using an equally weighted double exponential upon the belief that the extreme nonexponential behavior was the result of the two labeled methyl group sites in the dodecamer experiencing different motional environments. This resulted in $\langle T_1 \rangle$ values of 921 and 107 ms for the equally weighted biexponential fit and in a $\langle T_1 \rangle$ of 357 ms for a single-exponential fit, compared to the $\langle T_1 \rangle$ of 1.08 s observed for the dry monomer. Relaxation recovery for all remaining humidities investigated were fit by using a single exponential. The biexponential behavior of the dry sample may reflect differences in local environment between the monomer [*methyl*-^2H]thymidine and the dodecamer, but these differences were not pursued further.

Discussion

Analysis of NMR powder line shapes has provided insight into the internal dynamics of DNA. Numerous models have been presented to explain various aspects of previous ^2H and ^{31}P solid-state NMR studies (Fujiwara & Shindo, 1985; Brandes et al., 1986, 1988a, 1990; Shindo et al., 1987). The general procedure is to consider several different models, simulate the resulting NMR spectrum, and compare to the experimentally observed line shape. Line-shape analysis can never prove that a model represents what is physically occurring in the system, but analysis of experimental line shapes can dismiss certain models. It is hoped that a model can be developed that accounts for all attributes of the line shape and relaxation data and is compatible with studies involving labeling at different sites.

The first characteristic of the line shape considered was the variation in QCC_{eff} and η_{eff} with increasing humidity. The simplest model considered consists of a rapid 3-fold jump about the C_3 symmetry axis of the methyl group. A motionally averaged line shape characteristic of fast methyl reorientation was observed in the dry dodecamer and monomer samples. To describe the methyl group dynamics in monomer studies of [*methyl*-^2H]thymidine (Kintanar et al., 1988), the 3-fold-jump model was found to be superior to a model of free diffusion about the C_3 axis and was subsequently used to describe the methyl motion within the dodecamer. Increasing the rate of the methyl motion will not alter the line shape, the observed line shape being in the rapid narrowing regime. This places a lower limit on the rate responsible for the spectral line shape observed, $\tau_c \ll \omega_Q^{-1} \sim 10^{-6}$ s. This conclusion is also supported by the observation that varying the interval τ_1 in the quadrupolar echo sequence from 40 to 200 μs produces little intensity loss and no distortion of the powder line shape. The short anisotropic T_{2e} effects expected for motions occurring in the intermediate regime were not observed in the dry sample. The reduction in QCC_{eff} could occur due to variation in β, which describes the angle between the methyl motional axis and the q_{zz} element of the EFG tensor, which is typically oriented coincident with the carbon–deuterium bond. This explanation has been used to describe the reduction in QCC_{eff} in studies of polycrystalline amino acids (Batchelder et al., 1983). However, to explain the large reductions in QCC_{eff} that occur at high hydration levels, a distortion of the tetrahedral configuration of the methyl group to $\beta = 43°$ would be required. Such a large variation in β was considered physically unrealistic and was not pursued further. All subsequent analysis assumed $\beta = 70.5°$, and any reduction in QCC_{eff} was attributed to additional averaging of the quadrupolar tensor by internal or overall motions.

Incorporation of a 2-fold libration of the base plane in addition to the methyl group 3-fold jump was also considered. This model was evaluated previously in the dynamic studies of thymidine monomer as well as analysis of the base-labeled dodecamer (Kintanar et al., 1988, 1989). Since the methyl group 3-fold-jump motion produces an axially symmetric averaged tensor, the direction of the 2-fold libration cannot be assigned, the averaged elements of the methyl EFG tensor being equivalent ($\bar{q}_{xx} = \bar{q}_{yy}$). Directional analysis has been discussed for other base studies (Shindo et al., 1987; Brandes et al., 1988a,b), the relative orientation of the EFG tensor in the molecular frame being obtained from analysis of oriented DNA samples. In the analysis of ^2H base labeled purine studies, it has been found that q_{xx} of the EFG tensor lies approximately in the base plane, but the present study involves the analysis of the methyl EFG tensor and no direct comparison is applicable.

The reduction in QCC_{eff} at 75% RH and 80% RH can be accounted for by increasing the angle of libration from $\theta = 9°$ for the dry sample to $\theta = 12°$ at 80% RH (W = 11.6), both at a rate with $\tau_c < 10^{-6}$ s, where θ is the half-angle between the two sites. This is in agreement with the [H6-^2H]thymidine studies in the same dodecamer (Kintanar et al., 1989). It is interesting to consider correlation times (τ_c) calculated from corresponding $\langle T_1 \rangle$ values for this model. Spin–lattice relaxation behavior for a model including a 3-fold jump about the C_3 symmetry axis and an uncorrelated small-amplitude 2-fold libration was determined with an expression (Alam, unpublished results) based on the two-axis correlation function

$$C_{aa'}(t) = \sum_{bb'=-2}^{2} (-1)^{b-b'} d^{(2)}_{ba}(\theta) d^{(2)}_{b'a}(\theta) d^{(2)}_{0b}(\beta) d^{(2)}_{0b}(\beta) \Gamma^{Me}_{bb'}(t) \Gamma^{Lib}_{bb'aa'}(t)$$

where β is the angle between the q_{zz} axis of the EFG tensor in the principal axis system and the methyl symmetry axis,

θ describes the relative orientation of the methyl symmetry axis and the librational symmetry axis, and $d^{(2)}_{mn}$ values are elements of the Wigner rotation matrix (Brink & Satchler, 1968). The correlation function for the methyl group three-site jump, $\Gamma^{Me}_{bb'}(t)$, has been previously described (Torchia & Szabo, 1982). The correlation function for the two-site libration model, $\Gamma^{Lib}_{bb'aa}(t)$, was obtained by using a jump model formalism (Wittebort & Szabo, 1978; Torchia & Szabo, 1982) and was simplified by considering power average $\langle T_1 \rangle$ expressions. (The correlation function retains only those terms $a = a'$.) For $\theta = 12°$ and $\beta = 70.5°$, four solutions are obtained for the correlation time. The 2-fold libration has solutions for the correlation time, τ_c, of $\sim 3.6 \times 10^{-8}$ or $\sim 4.6 \times 10^{-11}$ s, with the corresponding pair of methyl solutions, $\tau_c \sim 1.5 \times 10^{-7}$ or $\sim 1.3 \times 10^{-11}$ s. The pair of solutions with slower methyl correlation times do not reproduce the experimental methyl fast averaged line shape. On the other hand, both solutions for τ_c of the librational motion result produce nearly identical methyl line shapes regardless of pulse spacing, τ_1. Simulations of base-labeled line shapes for the librational correlation time solutions show only minor variation in center intensity. Given the signal to noise ratio observed for the base-labeled material at 80% RH (Kintanar et al., 1989), it would be difficult to distinguish between these two solutions. In contrast, analysis of the dry base-labeled dodecamer $\langle T_1 \rangle$ produces librational correlation time solutions with distinguishable line shapes, supporting the assumption that the correct librational correlation time is on the fast side of the T_1 curve. Additional information is available from relaxation studies at different field strengths which are presently in progress.

Attempts to extrapolate this two-site librational model to 88% RH (**W** = 16.3) and beyond were unsuccessful. Increasing the angle of libration to account for reduction in QCC_{eff} resulted in a dramatic increase in η_{eff}. This was not observed experimentally, suggesting that a 2-fold jump model is unrealistic in describing the internal dynamics of the base. A similar conclusion was reached in the analysis of relaxation rates in oriented fibers (Brandes et al., 1990), where similar T_1 relaxation rates for $\Theta = 90°$ and $= 0°$ suggests the bases undergo a more symmetric motion.

Different models have been proposed to describe internal motions in DNA (Lipari & Szabo, 1981a). The diffusion-in-a-cone model (Warchol & Vaughan, 1978; Wang & Pecora, 1980; Lipari & Szabo; 1981b) has found a wide range of applications including investigations of fluorescence polarization decay in membranes (Kinosita et al., 1977) and nuclear magnetic relaxation in lipids (Brainard & Szabo, 1981). It has also been used in the analysis of ^2H studies of purine-labeled nucleic acids (Brandes et al., 1986, 1990). Use of this model to describe the restricted motion of the base may not be completely applicable to the present study due to observation of $\eta_{eff} > 0$. A symmetric motion like diffusion in a cone, along with the methyl 3-fold jump motion, will produce a symmetrically averaged EFG tensor ($\eta_{eff} = 0$), but use of this model, ignoring deviations from axial symmetry of the molecular motion, still allows an estimation of changes in internal motion with increasing hydration. Defining θ_0 as the half-angle of the cone in which the C_3 symmetry axis is allowed to freely diffuse and ignoring the small asymmetry parameter, the effective quadrupolar coupling constant is given approximately by

$$QCC_{eff} \sim (e^2qQ/h)^{Me}_{eff} S_{zz}$$

where $(e^2qQ/h)^{Me}_{eff}$ is the effective averaged quadrupolar coupling constant due to rapid methyl motion, and the uniaxial order parameter for diffusion in a cone is given by

$$S_{zz} = (\cos \theta_0 + \cos^2 \theta_0)/2$$

Assuming that there are no significant librational motions present within the dry-sample application of this diffusion-in-a-cone model gives $S_{zz} = 0.981$ and $\theta_0 = 9°$ at 80% RH, $S_{zz} = 0.883$ and $\theta_0 = 23°$ at 88% RH, $S_{zz} = 0.388$ and $\theta_0 = 59°$ at 92% RH, and $S_{zz} = 0.291$ and $\theta_0 = 65°$ at 95% RH. The value of 80% RH is smaller than the reported $\theta_0 = 16°$ for 84% RH in Li–DNA (Brandes et al., 1986), which has a similar water content. It compares well with the $\theta_0 = 8.5°$ reported for salmon DNA (Shindo et al., 1987). Analysis of purine base labeled dodecamer data with a diffusion-in-a-cone model resulted in similar values for the angle of fluctuation, with $\theta_0 = 17°$ at 80% RH and $\theta_0 = 57°$ at 92% RH. These values for θ_0 assumed that librational motions were absent in the dry methyl labeled dodecamer. Including the possibility of librational motions within the monomer and dry dodecamer will increase the angle of fluctuations. Besides the inability of this model to describe the intermediate rate line shape observed at 90% RH, the appearance of a nonzero asymmetry parameter and the large cone angle required to fit experimental spectra at elevated levels of hydration make the applicability of this model to the dodecamer data questionable. Additional models need to be investigated. Of course, a nonzero asymmetry parameter can be obtained by means other than through a nonsymmetric motion, but in accord with the model presented in the previous thymidine monomer studies, these were not considered [see Kintanar et al. (1988) for a further discussion].

A biaxial model, consisting of motions in two perpendicular directions, has been previously presented as a model of internal base motions (Brandes et al., 1986, 1988a; Shindo et al., 1987). In all cases it is assumed that one direction of libration is within the base-pair plane and the second direction of libration is perpendicular to that plane. The fluctuations of the methyl C_3 symmetry axis are described by ϕ_0 for the in-plane libration and by θ_0 for the out-of-plane librations. Relation of θ_0 and ϕ_0 to a specific direction with respect to the C_3 symmetry axis is not possible, since the methyl motion alone produces a symmetric averaged EFG. Assignment of which direction is θ_0 and which is ϕ_0 is possible from an analysis of the aligned liquid-crystal spectrum, which allows discrimination between twisting and tilting type motions, and will be treated in a future paper (Alam & Drobny, 1990). The changes in QCC_{eff} and η_{eff} with increasing humidity can be described by increases in θ_0 and ϕ_0. By use of the static value of e^2qQ/h obtained from monomer studies, the line shape of the dry sample can be simulated by using $\theta_0 = 9° \pm 1°$, and $\phi_0 = 7° \pm 1°$. At 75% RH (**W** = 10.4) and 80% RH (**W** = 11.6) the angles of libration increase to $\theta_0 = 12° \pm 2°$ and $\phi_0 = 10° \pm 2°$, while at 88% RH (**W** = 16.3) $\theta_0 = 19° \pm 2°$ and $\phi_0 = 17° \pm 2°$, at 92% RH (**W** = 26.6) θ_0 and $\phi_0 \sim 40° \pm 3°$, and at 95% RH (**W** = 39.8) θ_0 and $\phi_0 \sim 43° \pm 3°$. The lower hydration levels compare favorably with values reported for calf thymus Li–DNA (Brandes et al., 1986, 1988a), while the higher hydration levels show substantially higher values of libration than reported for salmon DNA fibers and films (Shindo et al., 1987). This increase may result from differences in the actual level of hydration or from differences in the helix axis motion as discussed below. Analysis of the base-labeled dodecamer (Huang, 1989) using this four-site librational model resulted in surprisingly large differences between θ_0 and ϕ_0 given the values of η_{eff} at lower hydration levels, but at 92% RH, θ_0 and ϕ_0 equaled about 38°, remarkably close to those values obtained for the methyl group. It should be noted that in the

methyl line shape analysis the angles are restricted to $\theta_0 \neq \phi_0$ to fulfill the requirement $\eta_{eff} \neq 0$.

If the librational motions of this four-site model are faster than the width of the rigid lattice spectrum, effective average values of QCC and η are produced. The correlation time of the libration cannot be determined from line-shape analysis, but an upper limit of $\tau_c < \omega_Q^{-1} \sim 10^{-6}$ s can be set. A thorough analysis of relaxation data is required for determination of τ_c; these experiments are in progress. The four-site librational model adequately fits the experimental line shape for dry and 66% RH (see Figure 2a). Comparison of simulated spectra for this model to experimental spectra at 75%, 80%, and 88% RH shows only partial agreement. The line shape observed at 90% RH, however, is characteristic of motion occurring in the intermediate rate regime and cannot be reproduced by fast librations regardless of angle. The angle of libration of $\sim\pm45°$ for 92% RH and higher hydration levels is again physically debatable. It is obvious that additional motions are occurring and that other line-shape characteristics must be addressed in the analysis of spectra. One characteristic to consider is the loss in center intensity with increasing humidity. This orientationally dependent attenuation is not present in the simulations involving only methyl motions and fast librations. Also observed is a loss in signal intensity or echo attenuation with variation in pulse spacing (see Figure 3a), as well as variation in relative intensity between hydration levels. The biaxial model consisting of only fast motions shows no variation in τ_1, nor can the simple increase in the librational angle account for the loss in signal intensity. The loss in intensity and line-shape modulation with respect to pulse spacing, τ_1, may be attributed to heteronuclear dipolar dephasing (Heaton et al., 1989). Consideration of these heteronuclear dipolar interactions with surrounding protons in the DNA and water molecules is impractical, requiring knowledge of each interaction distance. Recognizing the omission of heteronuclear dipolar contributions as an approximation, these effects were not considered further. If the spectra are scaled to the apparent $\langle T_{2e} \rangle$ present from interactions at dry or 66% RH, additional changes in T_{2e} with increasing humidity can be entirely attributed to dynamic processes within the oligonucleotide.

Changes in the observed experimental line shape can be accounted for by the appearance of a slower motion about the helix axis. Different models have been presented to describe the motion about the long axis of DNA (Allison & Schurr, 1979; Lipari & Szabo, 1981a); the simplest is to treat the DNA molecule as a rigid cylinder undergoing free diffusion or restricted diffusion about the helix axis. Coupling of the biaxial librational model with slow motion about the helix axis adequately reproduces the observed line shapes through 90% RH (W = 21.2). The effect of helix diffusion was simulated by using a jump model between nearest neighbors of equal site probability described by the equilibrium

$$S_1 \overset{k}{\rightleftharpoons} S_2 \overset{k}{\rightleftharpoons} \dots \overset{k}{\rightleftharpoons} S_n$$

where S_i represents the ith site and k represents the rate of jumping between sites. This type of model has been used in the analysis of ^2H and ^{31}P line shapes in DNA (Fujiwara & Shindo, 1985; Shindo et al., 1987; Kintanar et al., 1989). The relationship between k and the planar diffusion coefficient D_R can be obtained in the following manner. The number of random jumps required for an axis to reorient by an angle ξ is given by (Luz et al., 1981)

$$n_\xi = \xi^2/\theta_{ij}^2$$

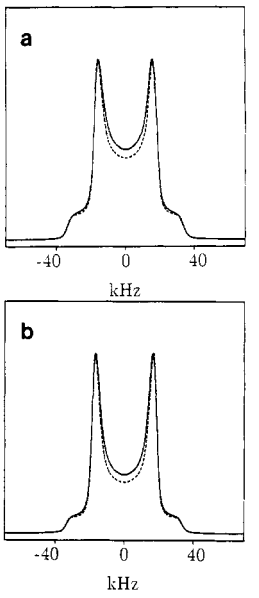

FIGURE 4: Simulated quadrupole echo spectra as a variation of N, the number of sites in the helix motion. (a) $\tau_1 = 50$ μs for 3 kHz, $\theta_{ij} = 20°$, (—) $N = 6$, (---) $N = 16$. (b) Same as (a) except $\tau_1 = 200$ μs. Note Figure 2c (---) is equal to (a) (—).

where θ_{ij} is the arc angle between successive sites. The average time required to reorient the axis by one radian is

$$\tau = n_1/k = 1/k\theta_{ij}^2$$

which can be used to obtain the diffusion coefficient

$$D_R = 1/2\tau = k\theta_{ij}^2/2$$

The larger the number of sites N, or the smaller the jump size θ_{ij}, the closer to the true diffusion limit this becomes. Studies by Wittebort and co-workers (1987) showed that differences in line shapes and variation in relative intensities can occur with increasing number of sites. The six-site jump model was used almost exclusively as a model of diffusion about the helix axis in the present simulations primarily to minimize computational time, but results are also presented for larger numbers of sites.

The experimental line shapes of 75% RH and 80% RH are simulated well by using the methyl rapid 3-fold jump, a fast four-site libration of the base plane, and a slower six-site helix motion at $k = 1$ kHz, $\theta_{ij} = 5°$ (see Figures 2b and 3c,d), corresponding to a $D_R = 3.8$ s^{-1}. Line-shape variations are minimal in going from $N = 6$ to $N = 16$ for the 1-kHz model, corresponding to total angular displacements of 25° and 75°. This suggests that the slow azimuthal rotation may not be truly restrictive in nature but at a rate slow enough to appear restricted in nature on a ^2H NMR time scale. The observed spectrum at 88% RH is fit similarly with $k = 3$ kHz, $\theta_{ij} = 20°$, corresponding to $D_R = 1.8 \times 10^2$ s^{-1}. Variations in the line shape for $N = 6$ and $N = 16$ are shown in Figure 4, corresponding to total angular displacements of 100° and 300°, respectively. There are minor differences with variation in N, but only small changes in the rate or angle would be required to fit the experimental spectra. The observed signal to noise ratio at 88% RH allowed only an approximate fit, but it was obvious from analysis of line-shape changes with variation in pulse spacing that the lack of anisotropic attenuation precludes models containing significantly larger angles and/or increased rates, since these produced line shapes that varied differently with interpulse spacing than was observed experimentally.

The experimental line shapes become difficult to interpret at higher hydrations due to local internal librations being

masked by larger amplitude motions occurring at low rates. Simulation of the intermediate line shape observed at 90% RH by using $\theta_{ij} = 60°$ and $k = 400$ kHz, corresponding to $D_R = 2.2 \times 10^5$ s^{-1} (with the amplitude of the four-site libration unchanged from that of 88% RH), produced line shapes with the same general characteristics, but insufficiently narrowed. Simulations where the rate or angle was varied from these values tended to produce line shapes uncharacteristic of the intermediate regime. An approximate fit can be obtained by increasing the internal fluctuations to θ_0 and $\phi_0 = 22°$ to give a librationally averaged $QCC_{eff} \sim 40$ kHz and $\eta_{eff} \sim 0$. One can also assume that those local motions described by the rapid 4-fold libration remain unchanged at hydration levels greater than 88% RH and that all subsequent variations in line shape result from motions in addition to the base libration. This is not entirely implausible in that at **W** = 16.3 the hydration of the oligonucleotide is complete. Between **W** = 5 and **W** = 12 the nucleotide bases are hydrated, above **W** = 12 the dodecamer is completely hydrated and additional water binds to the primary hydration level, and finally above **W** = 20 water adds to the grooves as well as between dodecamer helices (Falk et al., 1962, 1963a,b). Contributions of diffusion about an axis other than the azimuthal axis may also need to be considered. A rough estimate of contributions from diffusion about an axis perpendicular to the helix symmetry axis can be obtained from consideration of the rotational dynamics of circular cylinders and by using expressions applicable to shorter DNA fragments (Tirado & García de la Torre, 1980; Tirado et al., 1984). The ratio of diffusion rate about the helix axis and the axis perpendicular to the helix is approximately 1.9 for a molecule with a length to diameter aspect ratio of approximately 1.7. A rough simulation of the contributions from motion about an axis perpendicular to the helix axis can be obtained with this ratio. Simulation using a six-site jump motion about the helix axis at $k = 400$ kHz and $\theta_{ij} = 60°$, $D_{\parallel R} = 2.2 \times 10^5$ s^{-1}, and a helix "wobble" characterized by a three-site jump at $k = 1.56$ MHz, $\theta'_{ij} = 22°$, and $D_{\perp R} = 1.15 \times 10^5$ s^{-1} produced slightly improved fits of experimental spectra (see Figure 2d) compared to a simple reduction of QCC_{eff}. This jump model for helix wobble is a crude approximation for diffusional processes about two perpendicular axes, but it does demonstrate that increases in base libration may not be required to account for the additional narrowing. The possibility of magnetic ordering was investigated for 90% RH, but an aligned phase was not observed to be a major component at this hydration level.

Parameters obtained for the six-site jump model compare well to previous ^{2}H studies of DNA. Kintanar and co-workers analyzed the base-labeled dodecamer and found that at 80% RH $k = 3.3$ KHz, with $\theta_{ij} = 5°$, while at 88% RH $k = 1$ MHz, with $\theta_{ij} = 30°$. The lower humidity data correspond well with the values obtained from the methyl-labeled dodecamer, while the 88% RH data differ significantly. The rate and angle values reported by Kintanar and co-workers for 88% RH were investigated but produced line shapes that were distinctly outside the intermediate regime. This suggests that the methyl label is a more sensitive probe of motions occurring near 50 kHz. Applying this model to longer pieces of DNA at 92% RH, Shindo and co-workers found the best fit using $k = 2$ MHz, $\theta_{ij} = 30°$, corresponding to $D_R = 2.7 \times 10^5$ s^{-1}. This vlaue of D_R is surprisingly close to that observed at 90% RH, but simulations involving a restricted reorientation were unsuccessful, resulting in broad shoulderless methyl line shapes similar to those reported for the base. This discrepancy may be the result of the differences in DNA size, the smaller dodecamer being able to fully reorient about its helix axis at this hydration level. Above **W** ~ 25 the sample was found to align with the helix axis perpendicular to the magnetic field. Simulation of the line shapes observed at 92% RH (**W** = 26.6) and 95% RH (**W** = 39.9) can be obtained in a similar manner as described for lower hydration levels, except the degree of alignment must be considered. A more thorough investigation of this unique phase will be presented in a subsequent paper.

Analysis of the echo decay time, T_{2e}, allows investigation of motional rates occurring in the dodecamer, as well as a means of discriminating between various models. There have been numerous investigations of T_{2e} relaxation in lipids and integral membrane proteins (Davis, 1983; Pauls et al., 1985). Even though T_{2e} relaxation rates are angularly dependent, and therefore would give rise to nonexponential decay recovery curves, the signal to noise ratio for the deuterated dodecamer reported in this paper was not sufficient to detect these deviations from exponential behavior. Powder average decay rates (denoted $\langle T_{2e} \rangle$) were therefore determined and can be interpreted in terms of changes in the second moment of the observed line shape. The second moment, M_2, is given by

$$M_2 = \int_{-\infty}^{\infty} d\omega \omega^2 f(\omega) / \int_{-\infty}^{\infty} d\omega f(\omega)$$

where $\omega = 0$ is the Larmor frequency ω_0 and $f(\omega)$ is the line-shape function. For symmetric powder patterns the second moment can be related to the effective quadrupolar coupling constant by

$$M_2 \approx 9\pi^2 (QCC_{eff})^2 / 20$$

A qualitative analysis of T_{2e} relaxation shows that in the slow motional limit $T_{2e} \sim \tau_c$, while in the rapid limit $T_{2e} \sim (\tau_c \Delta M_2)^{-1}$ (Pauls et al., 1985). This shows that for a motion about a single axis variation in the correlation time from the slow or rigid limit to the rapid time scale results in T_{2e} passing through a minimum. Intepretation of T_{2e} for the dodecamer would require consideration of other internal dynamics in addition to motion about the helix axis, but the appearance of a T_{2e} minimum supports the model of an increase in the rate of motion about the helix axis with higher humidity levels as proposed from line-shape analysis. As a crude approximation of the correlation time for this rotational process, changes in the second moment can be related to the loss in quadrupole echo by

$$1/T_{2e} = \Delta M_2 \tau_c$$

For 92% RH the changes in the second moment (assuming that they result entirely from motion about the helix axis), give $\tau_c \sim 5 \times 10^{-7}$ s. This is a crude approximation of the correlation time of helix motion and is complicated by the fact that changes in the second moment may result from other motions occurring within the dodecamer. Analysis of T_{2e} can still be used to discriminate between various models, by comparison to decay rates obtained from simulations. These rates were scaled to the $\langle T_{2e} \rangle$ observed in the dry sample and represent relaxation due to motional changes in comparison to the dry sample. Simulated values of $\langle T_{2e} \rangle$ are given in Table I and compare favorably with those observed experimentally. In particular, the reversal of $\langle T_{2e} \rangle$ with increasing humidity levels is reproduced. Attempts to simulate the overall loss in echo intensity as a function of **W** from these models were not successful. The overall trend of signal intensity loss was observed, but the magnitude of echo attenuation was less than observed experimentally. This discrepancy may in part

be due to the numerous experimental conditions that can contribute to echo intensity attenuation or due to interactions (i.e., heteronuclear dipolar dephasing) not explicitly considered.

Conclusion

In summary, we have obtained ^2H NMR spectra of [*methyl*-^2H]thymidine-labeled [d(CGCGAAT*T*CGCG)]$_2$ as a function of hydration level. From line-shape analysis increases in hydration level lead to small but significant changes in the degree of librational fluctuations. At higher hydration levels there is the appearance of an additional motion about the helix axis which increases in rate with elevated water content. This helix motion must be included to account for the line shape observed at 90% RH. Analysis of variation in the methyl line shape has yielded a wealth of information on internal dynamics in the dodecamer at higher hydration levels than investigated in previous base-labeled studies. The methyl label has also proven to be an excellent probe of slower helix motions occurring in the range of 20 μs. There still exist ambiguities about the nature of the helix motion, since the exact model to describe this motion cannot be readily determined from powder line shape analysis. These ambiguities may be reduced by investigation of relaxation data, but the complexity of motions observed does not allow a simple intepretation of relaxation data, especially at a single field strength. Various models for motion about the helix axis have been proposed including free diffusion of a rigid rod and restricted diffusion within a square well potential or Gaussian potential, as well as diffusion models incorporating collective torsional modes. Careful analysis of spin–lattice and quadrupolar order relaxation as a function of field strength can provide a means of discriminating between these various models. Studies of the relaxation behavior of the methyl-labeled dodecamer at various field strengths are in progress and will be discussed in detail in a later publication. We are also investigating internal dynamics of the sugar and backbone of DNA by studying dodecamers labeled at the sugar 2″- or 5′- and 5″-positions. In addition, investigation of variation in internal dynamics with drug binding is underway.

Acknowledgments

We thank Dr. Paul Ellis, Dr. Regitze Vold, and Dr. Robert Vold for providing original copies of the simulation program MXQET and for sending us a preprint of the Brandes et al. (1990) paper. We thank Susan Ribeiro for her technical assistance in the oligonucelotide synthesis. We also thank Dr. Adreas Spaldenstein, Dr. John Orban, and Dr. Brian Reid for advice and material for the preparation of labeled compounds and Dr. Agustin Kintanar, Dr. Wen-Chang Huang, Dr. J. Michael Schurr, and Dr. Bruce Robinson for valuable discussions on DNA dynamics.

References

Abragam, A. (1961) in *Principles of Nuclear Magnetism*, pp 216–263, Oxford University Press, New York.

Alam, T. M., & Drobny, G. (1990) *J. Chem. Phys.* (in press).

Allison, S. A., & Shurr, J. M. (1979) *Chem. Phys. 41*, 35–59.

Allison, S. A., Shibata, J. H., Wilcoxon, J., & Schurr, J. M. (1982) *Biopolymers 21*, 729–762.

Barbara, T. M., Greenfield, M. S., Vold, R. L., & Vold., R. R. (1986) *J. Magn. Reson. 69*, 311–330.

Barkley, M. D., & Zimm, B. H. (1979) *J. Chem. Phys. 70*, 2991–3007.

Barone, A. D., Tang, J.-Y., & Caruthers, M. H. (1984) *Nucleic Acids Res. 12*, 4051–4060.

Batchelder, L. S., Niu, C. H., & Torchia, D. A. (1983) *J. Am. Chem. Soc. 105*, 2228–2231.

Bax, A., & Lerner, L. (1988) *J. Magn. Reson. 79*, 429–438.

Bendel, J., Laub, O., & James, T. L. (1982) *J. Am. Chem. Soc. 104*, 6748–6754.

Bendel, P., Boesch, J., & James, T. L. (1983) *Biochim. Biophys. Acta 759*, 205–213.

Bolton, P. H., & James, T. L. (1979) *J. Phys. Chem. 83*, 3359–3366.

Bolton, P. H., & James, T. L. (1980) *J. Am. Chem. Soc. 102*, 25–31.

Brainard, J. R., & Szabo, A. (1981) *Biochemistry 20*, 4618–4628.

Brandes, R., & Kearns, D. R. (1986) *Biochemistry 25*, 5890–5895.

Brandes, R., Vold, R. R., Vold, R. L., & Kearns, D. R. (1986) *Biochemistry 25*, 7744–7751.

Brandes, R., Vold, R. R., & Kearns, D. R. (1988a) *J. Mol. Biol. 202*, 321–332.

Brandes, R., Kearns, D. R., & Rupprecht, A. (1988b) *Biopolymers 27*, 717–732.

Brandes, R., Vold, R. R., Kearns, D. R., & Rupprecht, A. (1990) *Biochemistry 29*, 1717–1721.

Brink, D. M., & Satchler, G. R. (1968) in *Angular Momentum*, Oxford University Press (Clarendon), London.

Davis, J. H. (1983) *Biochim. Biophys. Acta 737*, 117–171.

De Fontaine, D. L., Ross, D. K., & Ternai, B. (1975) *J. Magn. Reson. 18*, 276–281.

Dickerson, R. E., & Drew, H. R. (1981a) *J. Mol. Biol. 149*, 761–786.

Dickerson, R. E., & Drew, H. R. (1981b) *Proc. Natl. Acad. Sci. U.S.A. 78*, 7318–7322.

DiVerdi, J. A., & Opella, S. J. (1981) *J. Mol. Biol. 149*, 307–311.

Drew, H. R., & Dickerson, R. E. (1981) *J. Mol. Biol. 151*, 535–556.

Drew, H. R., Wing, R. M., Takano, T., Broka, C., Tanaka, S., Itakura, K., & Dickerson, R. E. (1981) *Proc. Natl. Acad. Sci. U.S.A. 78*, 2179–2183.

Edzes, H. T., Ruppert, A., & Berendsen, H. J. C. (1972) *Biochem. Biophys. Res. Commun. 46*, 790–794.

Einarsson, L., Eriksson, P., Nordenskiöld, L., & Rupprecht, A. (1990) *J. Chem. Phys.* (submitted for publication).

Falk, M., Hartman, K. A., Jr., & Lord, R. C. (1962) *J. Am. Chem. Soc. 84*, 3843–3846.

Falk, M., Hartman, K. A., Jr., & Lord, R. C. (1963a) *J. Am. Chem. Soc. 85*, 387–391.

Falk, M., Hartman, K. A., Jr., & Lord, R. C. (1963b) *J. Am. Chem. Soc. 85*, 391–394.

Fujiwara, T., & Shindo, H. (1985) *Biochemistry 24*, 896–902.

Greenfield, M. S., Ronemus, A. D., Vold, R. L., & Vold, R. R. (1987) *J. Magn. Reson. 72*, 89–107.

Griffin, R. G. (1981) *Methods Enzymol. 72*, 108–174.

Hare, D. R., Wemmer, D. E., Chou, S.-H., Drobny, G., & Reid, B. R. (1983) *J. Mol. Biol. 171*, 319–336.

Heaton, N. J., Vold, R. R., & Vold, R. L. (1989) *J. Chem. Phys. 91*, 56–62.

Hogan, M. E., & Jardetzky, O. (1979) *Proc. Natl. Acad Sci. U.S.A. 76*, 6341–6345.

Hogan, M. E., & Jardetzky, O. (1980) *Biochemistry 19*, 3460–3468.

Holbrook, S. R., & Kim, S.-H. (1984) *J. Mol. Biol. 173*, 361–388.
Huang, W.-C. (1989) Ph.D. Thesis, University of Washington, June.
Huang, W.-C., Orban, J., Kintanar, A., Reid, B. R., & Drobny, G. P. (1990) *J. Am. Chem. Soc.* (submitted for publication).
James, T. L. (1984) in *Phosphorus-31 NMR Principles and Applications* (Gorenstein, D. G., Ed.) pp 349–400, Academic Press, New York.
James, T. L., Bendel, P., James, J. L., Keepers, J. W., Kollman, P. A., Lapidot, A., Murphy-Boesch, J., & Taylor, J. E. (1983) in *Nucleic Acids: The Vectors of Life* (Pullman, B., & Jortner, J., Ed.) pp 155–167, Reidel Publishing, Dordrecht, Holland.
Kinosita, K., Kawato, S., & Ikegami, A. (1977) *Biophys. J. 20*, 289–305.
Kintanar, A., Alam, T. M., Huang, W.-C., Schindele, D. C., Wemmer, D. E., & Drobny, G. (1988) *J. Am. Chem. Soc. 110*, 6367–6372.
Kintanar, A., Huang, W.-C., Schindele, D. C., Wemmer, D. E., & Drobny, G. (1989) *Biochemistry 28*, 282–293.
Kopka, M. L., Frantini, A. V., Drew, H. R., & Dickerson, R. E. (1983) *J. Mol. Biol. 163*, 129–146.
Kopka, M. L., Yoon, C., Goodsell, D., Pjura, P., & Dickerson, R. E. (1985) *J. Mol. Biol. 183*, 553–563.
Kowalewski, J., Einarsson, L., Nordenskiöld, L., & Rupprecht, A. (1988) *J. Magn. Reson. 76*, 337–340.
Langowski, J., Fujimoto, B. S., Wemmer, D. E., Benight, A. S., Drobny, G., Shibata, J. H., & Schurr, J. M. (1985) *Biopolymers 24*, 1023–1056.
Lipari, G., & Szabo, A. (1981a) *Biochemistry 20*, 6250–6256.
Lipari, G., & Szabo, A. (1981b) *J. Chem. Phys. 75*, 2971–2976.
Luz, Z., Poupko, R., & Samulski, E. T. (1981) *J. Chem. Phys. 74*, 5825–5837.
Nerdal, W., Hare, D. R., & Reid, B. R. (1989) *Biochemistry 28*, 10008–10021.
Opella, S. J. (1986) *Methods Enzymol. 131*, 327–361.
Opella, S. J., Wise, W. B., & DiVerdi, J. A. (1981) *Biochemistry 20*, 284–290.
Pauls, K. P., MacKay, A. L., Söderman, O., Bloom, M., Tanjea, A. K., & Hodges, R. S. (1985) *Eur. Biophys. J. 12*, 1–11.
Pjura, P. E., Grzeskowiak, K., & Dickerson, R. E. (1987) *J. Mol. Biol. 197*, 257–271.
Roy, S., Hiyama, Y., Torchia, D. A., & Cohen, J. S. (1986) *J. Am. Chem. Soc. 108*, 1675–1678.
Rupprecht, A., & Forslind, B. (1970) *Biochim. Biophys. Acta 204*, 304–316.
Schurr, J. M., & Fujimoto, B. S. (1988) *Biopolymers 27*, 1543–1569.
Shindo, H. (1984) in *Phosphorus-31 NMR Principles and Applications* (Gorenstein, D. G., Ed.) pp 401–422, Academic Press, New York.
Shindo, H., Hiyama, Y., Roy, S., Cohen, J. S., & Torchia, D. A. (1987) *Bull. Chem. Soc. Jpn. 60*, 1631–1640.
Sinha, N. D., Biernat, J., McManus, J., & Köster, H. (1984) *Nucleic Acids Res. 12*, 4539–4557.
Spiess, H. W. (1985) *Adv. Polym. Sci. 66*, 23–58.
Ti, G. S., Gaffney, B. L., & Jones, R. A. (1982) *J. Am. Chem. Soc. 104*, 1316–1319.
Tirado, M. M., & García de la Torre, J. (1980) *J. Chem. Phys. 73*, 1986–1993.
Tirado, M. M., Martinez, C., & García de la Torre, J. (1984) *J. Chem. Phys. 81*, 2047–2052.
Torchia, D. A., & Szabo, A. (1982) *J. Magn. Reson. 49*, 107–121.
Vold, R. R., Brandes, R., Tsang, P., Kearns, D. R., & Vold, R. L. (1986) *J. Am. Chem. Soc. 108*, 302–303.
Wang, C. C., & Pecora, R. (1980) *J. Chem. Phys. 72*, 5333–5340.
Warchol, M. P., & Vaughan, W. E. (1978) *Adv. Mol. Relaxation Interact. Processes 13*, 317–330.
Weast, R. C. (1979) in *Handbook of Chemistry and Physics*, 60th ed., p E-46, CRC, Boca Raton, FL.
Wing, R., Drew, H., Takano, T., Broka, C., Tanaka, S., Itakura, K., & Dickerson, R. E. (1980) *Nature 287*, 755–758.
Wittebort, R. J., & Szabo, A. (1978) *J. Chem. Phys. 69*, 1722–1736.
Wittebort, R. J., Olejniczak, E. T., & Griffin, R. G. (1987) *J. Chem. Phys. 86*, 5411–5420.